



High-energy electrons from the muon decay in orbit: Radiative corrections



Robert Szafron*, Andrzej Czarnecki*

Department of Physics, University of Alberta, Edmonton, Alberta T6G 2G7, Canada

ARTICLE INFO

Article history:

Received 27 October 2015

Received in revised form 29 November 2015

Accepted 3 December 2015

Available online 7 December 2015

Editor: B. Grinstein

ABSTRACT

We determine the $\mathcal{O}(\alpha)$ correction to the energy spectrum of electrons produced in the decay of muons bound in atoms. We focus on the high-energy end of the spectrum that constitutes a background for the muon–electron conversion and will be precisely measured by the upcoming experiments Mu2e and COMET. The correction suppresses the background by about 15%.

© 2015 The Authors. Published by Elsevier B.V. This is an open access article under the CC BY license (<http://creativecommons.org/licenses/by/4.0/>). Funded by SCOAP³.

In matter, muons decay differently from antimuons. Although the decay rates are very similar [1], negatively charged μ^- can bind with nuclei. The nucleus exchanges photons with the muon and the daughter electron, rearranging the energy distribution. In this paper we find how this rearrangement is affected by the real radiation and self-interaction on the muon–electron line. We predict the energy spectrum of the highest-energy electrons, interesting both theoretically and experimentally.

For a theorist, the muon decay is the simplest example with which to understand the gamut of binding effects, including the motion in the initial state, interplay of the binding and the self-interaction, and the recoil of the nucleus. Experimenters have recently studied the bound muon decay (decay in orbit, DIO) [2] with a precision sufficient to probe radiative corrections, later evaluated in [3]; however, these studies concern only the lower half of the spectrum, largely accessible also to a free muon.

Interestingly, the energy range of electrons produced in the DIO reaches to about twice the maximum possible in a free muon decay. When the muon decays in vacuum, momentum conservation requires that at least half of the energy be carried away by the neutrinos. In the DIO, the nucleus can absorb the momentum without taking much energy because it is so heavy.

The high-energy part is important for the upcoming searches for the ultra-rare neutrinoless muon–electron conversion, COMET in J-PARC [4] and Mu2e in Fermilab [5]. Designed for a sensitivity better than one exotic conversion in 10^{16} ordinary muon decays, they will collect large samples of events with high-energy electrons. A reliably predicted spectrum is needed to distinguish the

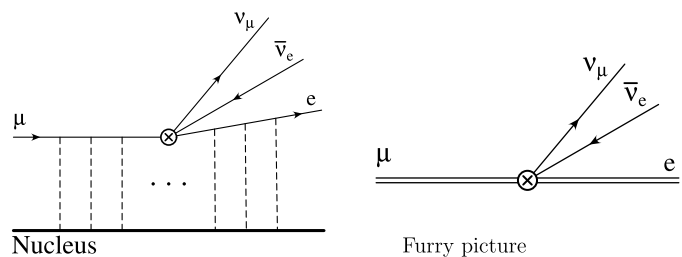


Fig. 1. Muon decay in orbit (DIO). Dashed lines denote Coulomb photons exchanged between charged leptons and the nucleus. The right panel shows the same physics using double lines for charged leptons propagating in the Coulomb field.

exotic signal – an excess of electrons at maximum energy – from the Standard Model background.

Predicting the DIO spectrum is a challenge because both the decaying muon and the daughter electron interact with the Coulomb field of the nucleus. A numerical calculation with Coulomb–Dirac wave functions is possible [6] provided that self-interactions (photons attached to the muon and the electron) are neglected. How can they be included? In the lower half of the spectrum the muon and the electron can be treated as nearly free and the binding effects can be factorized. Then the radiative corrections, known for a free muon, are convoluted with a shape function that parametrizes the Coulomb field effect [3,7]. Here we construct an expansion around the end-point and employ it to find radiative corrections also to the high-energy part of the spectrum.

Accounting for the external Coulomb field in charged-particle propagators is called the Furry picture [8]. In this formulation, and still ignoring radiative corrections, a single diagram, shown in Fig. 1, describes the DIO. We shall demonstrate that the bound-

* Corresponding authors.

E-mail address: andrzejc@ualberta.ca (A. Czarnecki).

state radiative corrections are easiest to evaluate near the high-energy end of the spectrum, the most important part for the new experiments. For now we neglect the nuclear recoil and structure, and treat the nucleus as an infinitely-heavy point source of the Coulomb field. We denote the electron energy with E ; its maximum value is $E_{\max} \simeq m_\mu \left(1 - \frac{(Z\alpha)^2}{2}\right)$, where m_μ is muon mass, Z is the atomic number, and $\alpha \simeq 1/137$ is the fine-structure constant. The DIO spectrum near its end-point can be expanded in the small parameter $\Delta = \frac{E_{\max} - E}{m_\mu}$,

$$\frac{m_\mu}{\Gamma_0} \frac{d\Gamma}{dE} = \sum_{ijk} B_{ijk} \Delta^i (\pi Z\alpha)^j \left(\frac{\alpha}{\pi}\right)^k, \quad (1)$$

where $\Gamma_0 = \frac{G_F^2 m_\mu^5}{192\pi^3}$ is the free-muon decay rate and G_F is the Fermi constant [9,10]. Powers of $\pi Z\alpha$ parameterize photon exchanges with the nucleus and α/π arises from radiative corrections on the charged-lepton line and the vacuum polarization. The first non-vanishing term has $i = j = 5$ and $k = 0$, with $B_{550} = \frac{1024}{5\pi^6} \simeq 0.21$. Higher order coefficients B may have logarithms of Δ and $Z\alpha$. The latter are a reminder that we are dealing with a decay in a Coulomb field, although the momentum transfer with the nucleus is sufficiently large that an expansion in $Z\alpha$ is possible. This is in contrast with the lower half of the spectrum, accessible with small momentum transfers, where binding effects cannot be treated perturbatively. The spectrum is a smooth function of Δ near the end-point, far from resonances.

Corrections to the leading behavior have several sources. The large momentum transfer to the nucleus probes its interior. The finite nuclear size, already included in [6], causes the largest correction. We will comment at the end of this paper on how to include it in our formalism. The finite nuclear mass introduces a recoil effect, also evaluated in [6]. It affects the coefficients B only slightly but it shifts the end-point energy E_{\max} .

We shall exploit a theoretical similarity between the DIO and the photoelectric effect to control higher-order binding effects. They generate powers of $\pi Z\alpha$ [11,12] rather than $Z\alpha$. Indeed, a numerical evaluation for a point nucleus with $Z = 13$ (as in aluminum, the planned target in COMET and Mu2e) finds a -21% correction, consistent with $13\pi\alpha = 0.3$. Logarithmic enhancement starts with $(\pi Z\alpha)^7 \ln(Z\alpha)$. Fortunately, these large effects, slightly suppressed by the finite nucleus size, are summed up in the numerical evaluation [6].

Finally, the most challenging corrections result from radiative effects that are the subject of this study. Before delving into the physics of the end-point, we present our main result. Close to the end-point, including radiative corrections, the DIO spectrum for aluminum is

$$\frac{m_\mu}{\Gamma_0} \frac{d\Gamma}{dE} \approx 1.24(3) \times 10^{-4} \times \Delta^{5.023}. \quad (2)$$

To illustrate the importance of the new corrections we consider the last 150 keV of the spectrum (the typical planned resolution of Mu2e and COMET). Radiative corrections reduce the number of events in this bin by 15%, a welcome reduction of the background, comparable in size with higher-order binding effects.

In the remainder we explain the origin of such a large effect. We begin with the tree-level behavior, appropriately expanding the lepton wave functions. We find that an exchange of a single, highly virtual photon gives the electron an energy of the full muon mass.

The asymptotic state of a relativistic electron with four-momentum p is described by a plane wave distorted by the Coulomb potential V . To the first order in V , in momentum representation indexed by \vec{q} , it is

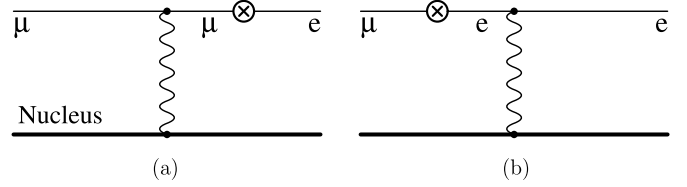


Fig. 2. Furry diagram expanded in $Z\alpha$. Crossed circles indicate insertions of the weak interaction transforming the muon into an electron; the emitted neutrinos are not shown. These two amplitudes give rise to the highest-energy electrons.

$$\bar{u}(p) \left[\delta^3(\vec{p} - \vec{q}) + \gamma \left((\vec{p} - \vec{q})^2 \right) \frac{1}{q - m_e} \right], \quad (3)$$

where $u(p)$ is a spinor solution of a free Dirac equation and the four-potential in momentum space reads

$$V(\vec{k}^2) = \left(-\frac{Z\alpha}{2\pi^2 \vec{k}^2}, \vec{0} \right). \quad (4)$$

A muon bound to a nucleus with $Z \ll 137$ is nonrelativistic. Nevertheless, we will need the first relativistic correction to its wave function, just like in the classic analysis of the photoelectric effect [13],

$$\psi(\vec{q}) = \psi_{\text{NR}}(\vec{q}) \left(1 + \frac{\vec{q} \cdot \vec{\gamma}}{2m_\mu} \right) u(P), \quad (5)$$

where $\psi_{\text{NR}}(\vec{q}) = \frac{8\pi Z\alpha m_\mu \Psi(0)}{[\vec{q}^2 + (Z\alpha m_\mu)^2]^2}$ is the nonrelativistic momentum-space wave function of the 1S ground state with $\Psi(0) = \left(\frac{Z\alpha m_\mu}{\pi^{1/3}} \right)^{3/2}$; $u(P)$ is the four-spinor of a muon at rest, $P = (m_\mu, 0)$. Higher order corrections to eq. (5) are suppressed by $Z\alpha$.

We now consider separately the contributions of the two terms in the electron wave function (3). The delta function term forces the muon momentum in (5) to be large, $\vec{q} = \vec{p} \sim m_\mu$. Thus we neglect $Z\alpha m_\mu$ in the denominator of ψ_{NR} and find

$$\psi(\vec{q}) \approx (2\pi)^3 \Psi(0) \frac{1}{\vec{p} + \vec{q} - m_\mu} \gamma(\vec{q}^2) u(P). \quad (6)$$

This is visualized in Fig. 2a: the muon, before decaying, transfers momentum $\vec{q} \sim m_\mu$ to the nucleus through a hard space-like photon. It is here that the relativistic correction to the muon wave function is important.

The second term in (3) refers to an electron scattered on the nucleus. Now the muon momentum, not restricted to large values, has its typical bound-state size $\vec{q} \sim Z\alpha m_\mu$, negligible in comparison with $\vec{p} \sim m_\mu$. We use $\lim_{a \rightarrow 0} \frac{8\pi a}{(q^2 + a^2)^2} = (2\pi)^3 \delta^3(\vec{q})$ to approximate the muon wave function,

$$\psi(\vec{q}) \approx (2\pi)^3 \Psi(0) \delta^3(\vec{q}) u(P). \quad (7)$$

This is shown in Fig. 2b, where the hard photon is exchanged after the decay.

The two diagrams in Fig. 2 add up to the leading contribution B_{550} in (1). In both cases any energy unused by the electron ($\sim \Delta$) is taken up by the neutrinos and not transferred to the nucleus. Counting neutrino momenta in the integrated matrix element explains the leading energy dependence in (1),

$$\int \frac{d^3 v}{v_0} \frac{d^3 \bar{v}_0}{\bar{v}_0} \delta(m_\mu \Delta - v_0 - \bar{v}_0) \dots \bar{v} \dots \bar{p} \sim \Delta^5. \quad (8)$$

Having understood that in the leading order in $Z\alpha$ only two diagrams describe the end-point behavior, we are now ready to evaluate order $\mathcal{O}(\frac{\alpha}{\pi})$ radiative corrections. In the Furry picture there are two groups of virtual corrections, shown in Fig. 3, and

Download English Version:

<https://daneshyari.com/en/article/1850501>

Download Persian Version:

<https://daneshyari.com/article/1850501>

[Daneshyari.com](https://daneshyari.com)